

# Design of Aerosol Face Masks for Children Using Computerized 3D Face Analysis

Israel Amirav, MD,<sup>1,2</sup> Anthony S. Luder, MD,<sup>1</sup> Asaf Halamish, EngBSc,<sup>3</sup> Dan Raviv, PhD,<sup>4,5</sup> Ron Kimmel, DSc,<sup>4</sup> Dan Waisman, MD,<sup>6</sup> and Michael T. Newhouse, MD, MSc, FRCP(C)<sup>7</sup>

## Abstract

**Background:** Aerosol masks were originally developed for adults and downsized for children. Overall fit to minimize dead space and a tight seal are problematic, because children's faces undergo rapid and marked topographic and internal anthropometric changes in their first few months/years of life. Facial three-dimensional (3D) anthropometric data were used to design an optimized pediatric mask.

**Methods:** Children's faces ( $n=271$ , aged 1 month to 4 years) were scanned with 3D technology. Data for the distance from the bridge of the nose to the tip of the chin (H) and the width of the mouth opening (W) were used to categorize the scans into "small," "medium," and "large" "clusters."

**Results:** "Average" masks were developed from each cluster to provide an optimal seal with minimal dead space. The resulting computerized contour, W and H, were used to develop the SootherMask<sup>®</sup> that enables children, "suckling" on their own pacifier, to keep the mask on their face, mainly by means of subatmospheric pressure. The relatively wide and flexible rim of the mask accommodates variations in facial size within and between clusters.

**Conclusions:** Unique pediatric face masks were developed based on anthropometric data obtained through computerized 3D face analysis. These masks follow facial contours and gently seal to the child's face, and thus may minimize aerosol leakage and dead space.

**Key words:** inhaled therapy, clinical trial, children, face mask, face analysis

## Introduction

**D**ELIVERY OF AEROSOLIZED MEDICATIONS is an important application for the use of face masks particularly in the pediatric population. Masks for providing aerosol therapy appear in various shapes, dimensions, and materials. To the best of our knowledge, there is little evidence for the design of existing, generally available, pediatric masks that appear to have been developed empirically for adults and then simply reduced in size for use in children.<sup>(1)</sup> An example of the empirical basis for pediatric masks design is shown in Figure 1, taken from Shah *et al.*<sup>(2)</sup> Whereas the upper border of most

masks is applied to the nasal bridge, their lower borders are applied at various locations: the cleft between the lower lip and the chin, the tip of the chin, or below the chin. The issue of mask size, contour, adequate fit, and dead space is a particular problem in infants and very young children whose faces, in the first few months/years of life, undergo rapid and marked developmental change in all dimensions.

We have been unable to find any scientific evidence to support existing face mask design in this age group. As far as can be determined, the only currently available data with respect to the design of infant masks were obtained in order to develop airplane oxygen masks where, as part of the

<sup>1</sup>Pediatric Department, Ziv Medical Center, Bar-Ilan University, Safed, Israel.

<sup>2</sup>Pediatric Department, Faculty of Medicine, University of Alberta, Edmonton, Alberta, Canada.

<sup>3</sup>Technosaf Inc., Karkur, Israel.

<sup>4</sup>Department of Computer Sciences, Technion University, Haifa, Israel.

<sup>5</sup>Camera Culture Group, Media Lab, Massachusetts Institute of Technology, Cambridge, MA.

<sup>6</sup>Department of Neonatology, Carmel Medical Center and Faculty of Medicine, Technion, Haifa, Israel.

<sup>7</sup>Firestone Institute for Respiratory Health, St. Joseph's Hospital, McMaster University Faculty of Health Sciences, Hamilton, Ontario, Canada.

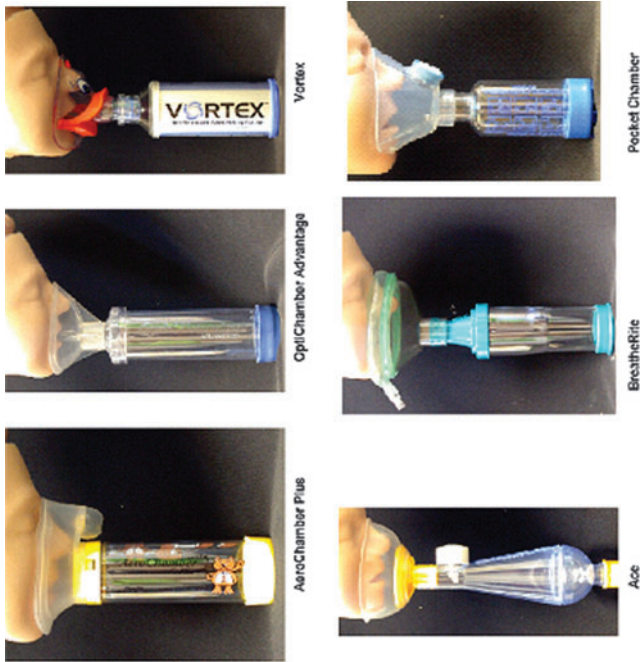


FIG. 1. Various masks supplied with valved aerosol holding chambers used for aerosol therapy. (Adapted with permission from Shah *et al.*<sup>2</sup>)

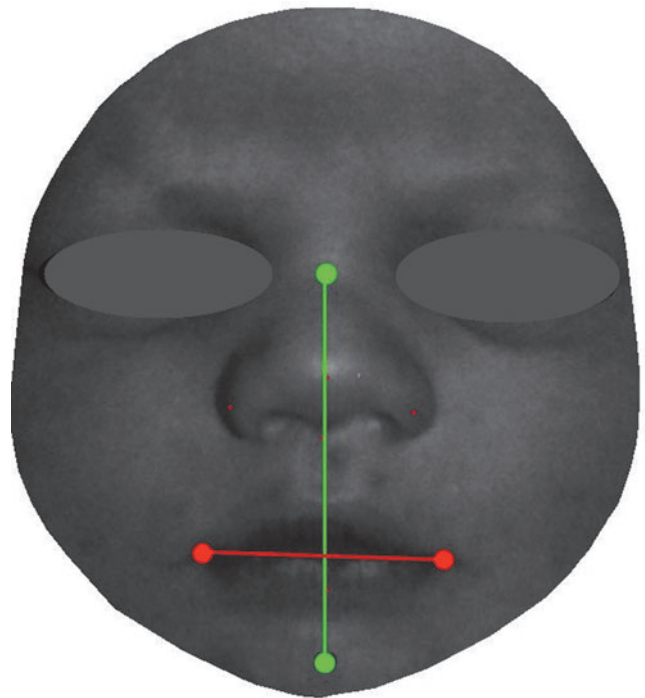


FIG. 5. Landmarks for facial measurements: nasal bridge to tip of the chin (green), and width of oral opening (red).

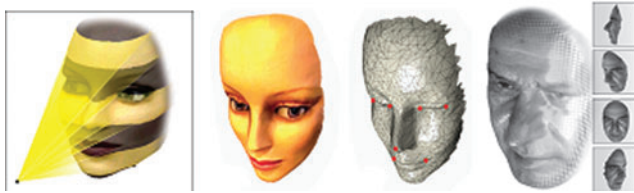


FIG. 2. Structured light and conversion to a triangulated surface or mesh. (Courtesy of Michael and Alex Bronstein.)



FIG. 3. Screen snapshots of 3D software results.

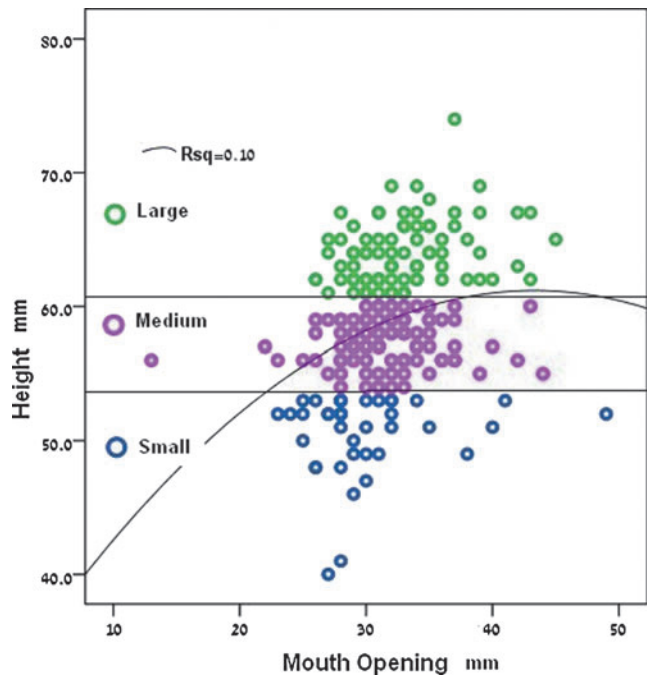


FIG. 6. Face height (H) versus mouth opening and three clusters (see text).

FIG. 4. Image acquisition. (Left to right) Camera; child in caregiver's lap; child looking to the left during image acquisition.



study of a full range of ages and facial dimensions, 40 infants' faces were evaluated.<sup>(3)</sup> Additionally, there exist some data about morphometric measurements of infants' faces with regard to possible surgical repair in various congenital anomalies (e.g., cleft palate<sup>(4-6)</sup>). However, there is no data set available that addresses mask design in infants, especially for aerosol delivery, where the fit and seal are of utmost importance if the aerosol dose is to be predictable, the dead space minimal, and the potential environmental and physical adverse effects, particularly due to leaks with nebulizers, minimized.<sup>(7,8)</sup>

This probably explains why current infant/toddler face mask design is suboptimal, particularly with regard to aerosol delivery where a tight seal is important to prevent leakage of drugs, such as aerosolized corticosteroids, toward the eyes. A tightly fitting mask is also necessary for minimizing leakage of potentially sensitizing agents, such as aerosolized antibiotics, into the caregivers' environment.

The aim of this study was to design a mask so that the alignment and seal between the facial surface contours and the mask can be optimized while minimizing mask dead space and maximizing comfort for the child. As developmental growth causes rapid changes in facial contours in the very young, it is clear that more than one size is needed while, at the same time, the number of mask sizes should be reasonable in order to facilitate prescribing by physicians. To achieve these goals, appropriate anthropometric data from the faces of infants and young children are needed. The present study describes our experience in obtaining anthropometric data with respect to the rapidly changing surface contours and increasing size of infants' faces during the first 4 years of life, data that were used to provide the basis for innovative face mask design for this age group.

## Materials and Methods

In the design process, we learned that the two key measurements for aerosol mask development are the dimensions of the mask in the coronal and sagittal planes and the contour of the mask rim where it seals to the face. From pilot experiments, we realized that the major factor influencing coronal dimensions of the mask is the vertical distance between surface features of the face, namely, the distance from the bridge of the nose to the tip (i.e., most anterior point) of the chin. These two landmarks were selected based on a literature search that found occasional references and recommendations suggesting that the use of these points was the single best predictor of a good seal.<sup>(2,3)</sup> Moreover, this distance was shown previously to undergo the greatest change with respect to growth, particularly in early life.<sup>(9)</sup>

Initial approaches included direct readings obtained from a simple ruler placed in front of the face or use of a digital camera to obtain images of the infant's face, while placing a ruler above or adjacent to the head followed by manual analysis of the photograph was recently reported successful in adults.<sup>(10)</sup> Both of these approaches failed due to infants' frequent movement during image acquisition.

We therefore adapted "face-analysis" software that was developed by the Computer Sciences Department at Technion University.<sup>(11,12)</sup>

This methodology is based on the evaluation of facial topographic three-dimensional (3D) photography. 3D surface imaging is rapidly replacing traditional "hands-on" anthropometry as the preferred method for quantifying topographic facial information.<sup>(13)</sup> Advantages of 3D imaging are minimal invasiveness, quick capture speeds, and the ability to archive images for subsequent analysis.<sup>(14)</sup> In addition, there is a high degree of precision and accuracy across a wide variety of 3D surface platforms.<sup>(15)</sup> The safety, speed, and reliability of data acquisition that 3D imaging offers are particularly helpful when working with young and unpredictably mobile children, in whom quantifying facial features can be particularly challenging.<sup>(13)</sup>

## Scientific basis of face analysis

In the past decade, considerable progress has been made in capturing and defining the geometric structure of 3D shapes. Stereovision and laser scanning are traditional techniques commonly used in such integrated systems. Laser scanners are relatively slow and require excessive processing power, whereas passive stereo systems have the disadvantage of dealing with a pair of images obtained simultaneously for which it is necessary to solve the difficult problem of image correspondence.

A nontriangulation technique that has recently been suggested is *time of flight*. It uses a camera that computes the time arrival profile of a pulse of a light. This technique is fast and can be inexpensively implemented.

The most popular classical technique, known as *structured light*, exploits the deformation of light patterns projected onto the object and calculates the depth using traditional triangulation. It is based on one or more specially designed light patterns projected onto the face, to obtain the 3D geometric structures. This technique is robust and accurate with submillimeter accuracy even for relatively textureless surfaces such as the human face (Fig. 2). We have optimized the system for increasing capture speed, modeling speed, accuracy, and cost. The light patterns are produced using a standard digital video projector controlled by a portable computer. The "range data" are converted digitally into a triangular surface mesh, and in a postscanning process, noise is removed and the holes in the surface are filled. The facial anthropometric structure of the 3D pictures is analyzed off-line using computerized face analysis software (Fig. 3).

## Subjects

The study was registered at ClinicalTrials.gov (NCT01274299). After obtaining the appropriate (Ziv Medical Center) Institutional Review Board approval and parental informed consent, we obtained 3D scans from 271 infants and young children. There were 144 boys and 127 girls.

Inclusion criteria included: age 1 month to 4 years, parental consent, and cooperation with the scanning procedure.

Exclusion criteria included: any kind of illness (per parents' report) in the week preceding enrollment and congenital facial anomalies.

Subjects were recruited from various nurseries on a voluntary and convenience basis.

Images were obtained in a quiet room with only the operator, caregiver, and child present (Fig. 4). Subjects were

usually seated on the lap of the caregiver (parent or day care personnel). Subjects (or the parent/caregiver) were positioned using a back support, and the seat's vertical height was adjusted to accommodate various heights. A constant distance between the subject and the camera was achieved using a meterstick from the camera's estimated focal plane to the child's forehead.

The geometric acquisition procedure included the following steps: calibration of the scanning system, wiping the child's face, capturing five to seven geometric scans per subject, and data acquisition/storage. The investigators previewed images at the time of image acquisition; if necessary, children were rescanned. To increase the likelihood of obtaining adequate data coverage, seven images were obtained sequentially for each subject. The entire imaging procedure was accomplished in less than 1 min.

Some of the children required devices such as toys with sound or lights to attract and maintain their attention in the preferred direction.

All scans were obtained at the nursery in the morning. Dimmed ambient light was used, and blinds covering the windows blocked direct sunlight. A suitable case allowed the camera assembly to be readily transported from nursery to nursery.

### Image analysis

An initial evaluation of each child's images was undertaken to ensure adequate images for further analysis. When reviewing the 3D images, we considered the following questions<sup>(13)</sup>:

- Was the subject's facial expression neutral?
- Was there evidence of unwanted motion during data acquisition?
- Was there evidence of interference by scalp hair or other artifacts that could impact image quality?
- Was the image quality satisfactory?
- Was there adequate surface coverage for the targeted facial regions?

Criteria for exclusion from further analysis were: crying, movement, moisture on the face, blurred image, loss of surface data, and image artifacts. Based on these criteria, 216 (of 271) infants were deemed appropriate for analysis (24 had missing demographic data, 29 had poor picture quality, 2 were judged outliers).

## Results

### Facial analysis

The vertical dimension (H) from lowest point on the bridge of the nose to the most protuberant point of the chin and the mouth horizontal "opening" distance (W) (between the two cheilions) provided the most reproducible measurements for our purposes (Fig. 5). Plots of H versus age demonstrated a highly variable and unpredictable relationship, which could not be of value for the purpose of mask design. However, when the data were plotted as H versus mouth opening (Fig. 6), a better and more predictive curve could be obtained. The data points in this plot were amenable to cluster analysis (see *Computational considerations* below). The data could potentially be divided into a number of groups or clusters. However, we concluded that three clusters were the most economical and practical for providing suitable masks for infants and young children. This approach seemed most likely to achieve our

design aims while providing appropriate convenience for the prescribing physician and/or pharmacist.

The geometric dimensions were thus used to provide three representative groups (small, medium, and large) using the K-means algorithm,<sup>(16)</sup> also known as the Max-Lloyd vector quantification technique.

**Computational considerations.** We refer to face indexed by  $i$  as an observation given by two numbers  $X_i = \{X_i^1, X_i^2\}$  describing distances between two feature points on the face.

The observations of  $n$  different faces are denoted by  $\{X_i \in R^2\}_{i=0}^n$ , where  $R^2$  is the Euclidean plane, and here, we consider only couples of positive numbers (distance measurements).

Next, the K-means algorithm's goal is to partition the observations into  $k$  sets  $S = \{S_1, S_2, \dots, S_k\}$  such that the sum of squared differences between each observation and the mean of its cluster is minimized. By denoting  $\mu_i$  the mean of  $S_i$ , we minimize

$$\min_s \sum_{i=1}^k \sum_{X_j \in S_i} \|X_j - \mu_i\|^2.$$

This approach provides  $k$  representatives for our data. One popular method used to solve this problem is an iterative technique, where each iteration involves two steps. First, we assume the centers are known, and cluster the sets according to proximity (partition into Vorovoi cells).

$$S_i = \{X_j : \|X_j - \mu_i\| \leq \|X_j - \mu_t\|, \forall j = 0, \dots, n, \forall t = 1, \dots, k\},$$

where the norm notation  $\|X_j - \mu_i\|$  measures the distance between vectors. Next, we assume the affiliation to clusters is known, and re-evaluate the center for each cluster by  $\mu_i = \frac{1}{|S_i|} \sum_{X_j \in S_i} X_j$ ,

where  $|S_i|$  is the number of the elements in the set  $S_i$  (size of the set). The K-means algorithm is efficient, practical, and converges, although not necessarily to the global minimum.

**Contour.** The 3D photographs were also used to obtain the contour of the mask rim applied to the facial contact plane. After the data were divided into three clusters by  $X^1 = H$  (vertical distance from the nasal bridge to the tip of the chin in mm) and the mouth opening horizontal distance ( $X^2 = W$ ), all faces within a cluster were precisely aligned to an *average* (representative) face model for the specific cluster using the iterative closest point (ICP) numerical algorithm. This is the method of choice for aligning geometric structures, particularly surfaces.<sup>(9,10)</sup>

Each 3D scan provides several thousand points in 3D space that serve as vertices of triangles that together form a triangulated mesh surface (Fig. 7A).

The ICP method starts with an initial "guesstimate" with regard to the position of one surface with respect to the other, and iteratively rotates and translates the surface for improving the alignment between the shapes.

Let us denote the  $n$  vertices  $\{P_i\}_{i=1}^n$  of the first mesh by  $P \in R^{3 \times n}$ , and the  $m$  vertices  $\{Q_i\}_{i=1}^m$  of the second mesh by  $Q \in R^{3 \times m}$ , and let  $R \in SO(3)$  denote the rotation and  $T \in R^3$  translation transformations. Note that  $R$  denotes a rotation

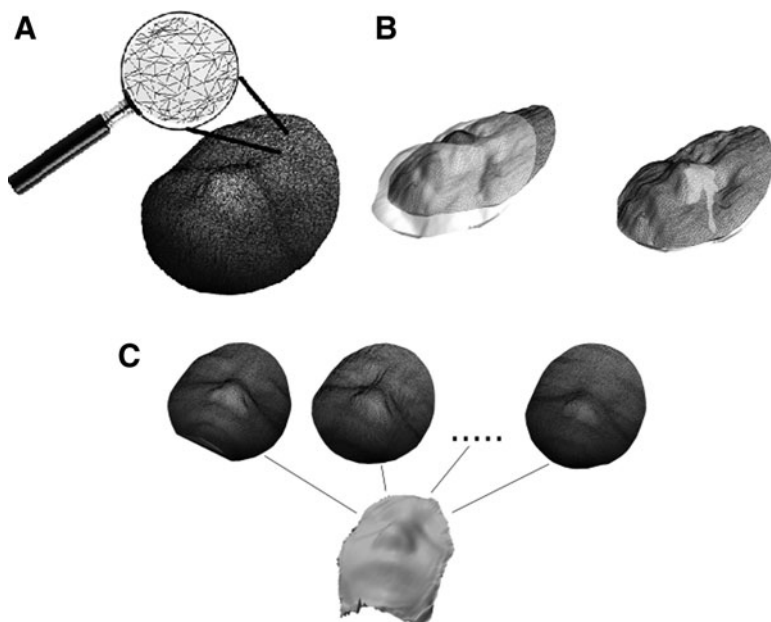


FIG. 7. (A) Triangulated mesh surface. (B) An example of the ICP procedure (see text). (C) A representative face is constructed by averaging the location of corresponding points for each cluster.

matrix in 3D space, and  $R^{3m}$  is Euclidean space of dimension  $3m$ . Our goal is to find a rigid transformation  $(R, T)$  that minimizes the distance between two surfaces given as point clouds  $P$  and  $Q$ . We search for the optimal transformation between the set of points, assuming the correspondence between the sets is provided. Our objective optimization is defined by

$$\arg \min_{R, T} \sum_{i=1}^n \|RP_i + T - Q_i\|.$$

It is solved by a convex optimization that provides a closed analytic solution for  $R$  and  $T$ . Next, we fix the position of the new set  $P'$  defined by  $P' = RP + P$  and compute the correspondence between the two new sets of points  $Q$  and  $P'$ . That is, for each  $P'_i \in P'$  we search for the closest  $Q_j \in Q$  in space. We then permute the indices of the points in  $Q$  such that for each  $P'_i$  its closest point in  $Q$  is  $Q_i$ . These two steps are iterated until convergence, again, not necessarily to the globally optimal solution if the initialization is not selected carefully. An example of the ICP procedure is illustrated in Figure 7B.

The two unaligned faces are shown on the left of the figure where one face is represented as a smooth template surface, and the second is represented as a triangulated mesh surface. The result of the alignment of these two faces, using the ICP numerical algorithm, is shown on the right of Figure 7B. After all faces were aligned, a representative face was constructed by averaging the location of corresponding points for each cluster (Fig. 7C).

#### The final design: small, medium, and large child masks

Using a specially designed software “engine” (SolidWorks, Waltham, MA), an appropriate mask was then hand drawn and fitted onto each of the “average” facial dimensions as shown in Figure 8A. Particular care was taken to ensure an optimally sealing mask with minimal dead space [e.g., 18 mL and 29 mL for the smallest and medium size

SootherMask<sup>®</sup> (SM) masks compared with 39 mL and 86 mL for the smallest and the medium AeroChamber masks]. The resulting mask contour was used to design the SM (Fig. 8B).

#### Discussion

The SM is a new concept of mask design, taking into account the needs of infants. It enables infants and young children, “suckling” on their own pacifier (or milk bottle nipple) inserted through a slot in the anterior surface of the mask, to create an effective and very gentle mask-to-face seal by means of subatmospheric pressure on the pacifier disc with little, if any, additional caregiver force application. The caregiver mainly assists in correctly aligning the mask to the facial contour.

Additional practical considerations must be taken into account. Most important, in our view, is what range of facial dimensions the three masks should appropriately cover and to what extent these dimensions should “overlap.” We focused on the vertical dimension, as it seemed to provide the most reliable and readily reproducible measurement. Taking into account the measured range and approximately 10% overlap between masks, we determined the final range to be from 45 to 80 mm. The first mask developed was the *small* unit. The mask was matched to the small cluster average face obtained from the ICP process. Taking into account the width of the mask rim as the sealing area, we designed the small mask so that it would cover all faces with the H dimension between 45 and 57 mm (Fig. 8C and Table 1).

The *medium* mask was developed from the medium cluster average dimensions to cover faces with H ranging from 55 to 69 mm (Table 1). This mask has a 2-mm overlap with the smallest mask. The *large* pediatric mask (Table 1) was developed from the large cluster average to cover faces with H ranging from 64 to 80 mm and provides a 5-mm overlap with the *medium* mask. All the subjects studied fit into either the small, medium, or large cluster. As the designed categories had some overlap, some of the subjects could be defined as being in two categories.

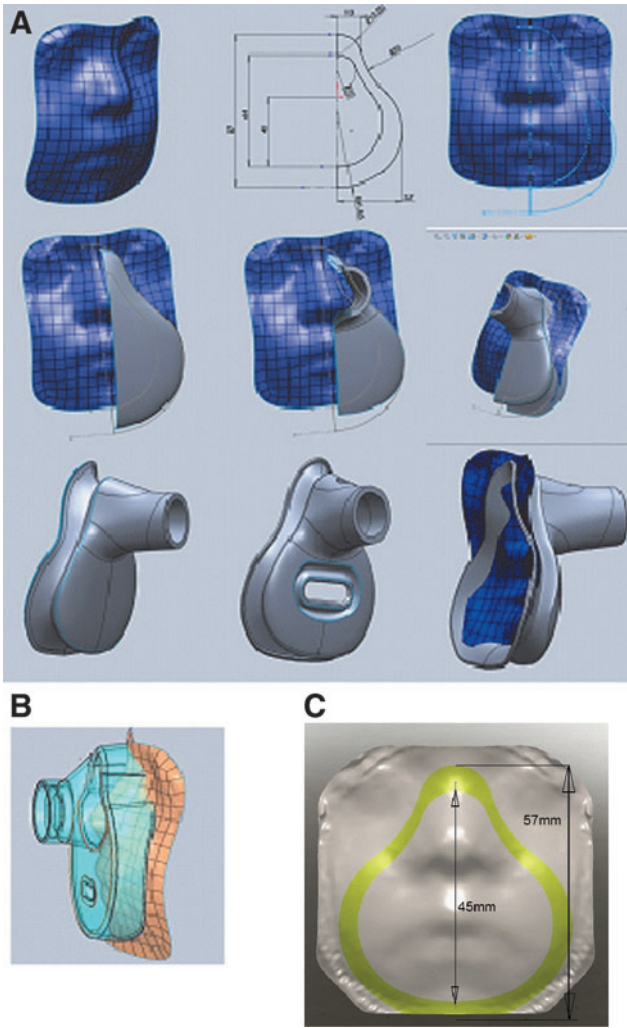


**FIG. 8.** (A) Design of a mask according to the facial contour. (B) Design of SootherMask with slot for the soother. (C) Designing the small mask to cover all faces with the H dimension between 45 and 57 mm.

### Limitations

Some limitations must be acknowledged. The generalizability of these dimensions to other races and/or congenital or acquired facial distortion is questionable and remains to be studied. The infants studied were of Western/Caucasian origin, and there may well be some ethnic variations and limitations.

**TABLE 1. MASK DIMENSIONS IN RELATION TO H (VERTICAL) MEASUREMENT**

Size	Height range <sup>a</sup> –open mouth (mm)	Height range <sup>b</sup> (mm)	Cover range (mm)	Overlap (mm)
Small	52–64	45–57	12	
Medium	62–76	55–69	14	2
Large	71–87	64–80	16	5

<sup>a</sup>All faces including those with their mouth open.

<sup>b</sup>All faces after subtracting mouth opening width.

The ICP algorithm may “smooth” the average representative face, and marked variations in facial contour have not been accounted for in the *average* dimensions resulting from these studies. Furthermore, outliers were excluded. To compensate for this, we have widened the overlap between the clusters so there is built-in overlap between different masks for faces of various sizes that may also compensate for ethnic variability. Additional studies may be needed and mask size/contour modifications undertaken if, as we undertake clinical validation studies, it appears that the masks are less than ideal for various racial features.

### Summary and Conclusions

Based on advanced 3D facial analysis techniques, evidence-based height and contour-fitting small, medium, and large masks have been developed for delivering aerosol therapies to infants, toddlers, and young children from birth to age 4 years. In contrast to currently available masks that have been developed empirically by simply scaling down adult mask dimensions, these masks are based on anthropometric data obtained through computerized 3D face analysis. They are designed to match facial sizes and follow facial contours and should gently seal to the child’s face. As 3D technologies are evolving, miniaturized, portable 3D scanners (possibly Smartphone apps) will possibly be used to facilitate the choice of mask size in the clinic. We are currently developing a simple proprietary device that will allow caregivers to rapidly determine the appropriate mask size for individual children.

### Acknowledgments

This research was partly supported by European Community’s FP7-ERC program, grant agreement no. 267414. Clinical Trial Registration is NCT01274299.

Dr. Amirav conceptualized and designed the study, coordinated and supervised data collection, drafted the initial manuscript, and reviewed and approved the final manuscript as submitted. Dr. Luder reviewed and approved the final manuscript as submitted. Mr. Halamish was involved in the study design, designed the data collection instruments, and coordinated and supervised data collection; he reviewed and approved the final manuscript as submitted. Dr. Raviv was involved in devising the geometric acquisition and shape analysis methodologies, the computational methods, and 3D software development, carried out the analysis, and reviewed and approved the final manuscript as submitted. Prof. Kimmel was involved in devising the geometric acquisition and shape analysis methodologies, the computational methods, and 3D software development, carried out the analysis, and reviewed and approved the final manuscript as submitted. Dr. Waisman was involved in the conception of the study, and reviewed and approved the final manuscript as submitted. Dr. Newhouse was involved in the study design and reviewed and approved the final manuscript as submitted.

### Author Disclosure Statement

Dr. Amirav and Dr. Newhouse have patents rights for devices for delivering aerosols to infants including those in the current study. Dr. Newhouse is the Chief Medical Officer of InspiRx Inc., developer of the SootherMask. The

other authors have no conflicts of interest relevant to this article to disclose.

## References

1. Amirav I, and Newhouse MT: Review of optimal characteristics of facemasks for valved-holding chambers (VHCs). *Pediatr Pulmonol.* 2008;43:268–274.
2. Shah SA, Berlinski AB, and Rubin BK: Force-dependent static dead space of face masks used with holding chambers. *Respir Care.* 2006;51:140–144.
3. Young JW: Selected facial measurements of children for oxygen-mask design. *AM 66-9. AM Rep.* 1966;1–11.
4. Cho BC, Kim JY, Yang JD, Chung HY, Park JW, and Hwang JH: Anthropometric study of the upper lip and the nose of infants less than a year of age. *J Craniofac Surg.* 2006;17:57–61.
5. Yamada T, Sugahara T, Mori Y, Minami K, and Sakuda M: Development of a 3-D measurement and evaluation system for facial forms with a liquid crystal range finder. *Comput Methods Programs Biomed.* 1999;58:159–173.
6. Yamada T, Mori Y, Minami K, Mishima K, and Tsukamoto Y: Three-dimensional analysis of facial morphology in normal Japanese children as control data for cleft surgery. *Cleft Palate Craniofac J.* 2002;39:517–526.
7. Geller DE: Clinical side effects during aerosol therapy: cutaneous and ocular effects. *J Aerosol Med.* 2007;20 Suppl 1:S100–S108; discussion S109.
8. Smaldone GC, Sangwan S, and Shah A: Facemask design, facial deposition, and delivered dose of nebulized aerosols. *J Aerosol Med.* 2007;20 Suppl 1:S66–S75; discussion S75–S77.
9. Bishara SE, Jorgensen GJ, and Jakobsen JR: Changes in facial dimensions assessed from lateral and frontal photographs. Part I—Methodology. *Am J Orthod Dentofacial Orthop.* 1995;108:389–393.
10. Zhang X, Hans M, Graham G, Kirchner HL, and Redline S: Correlations between cephalometric and facial photographic measurements of craniofacial form. *Am J Orthod Dentofacial Orthop* 2007;131:67–71.
11. Kimmel R: *Numerical Geometry of Images: Theory, Algorithms, and Applications.* Springer, New York; 2003.
12. Bronstein AM, Bronstein MM, and Kimmel R: *Numerical Geometry of Non-Rigid Shapes.* Springer, New York; 2008.
13. Heike CL, Upson K, Stuhaug E, and Weinberg SM: 3D digital stereophotogrammetry: a practical guide to facial image acquisition. *Head Face Med.* 2010;6:18.
14. Khambay B, Nairn N, Bell A, Miller J, Bowman A, and Ayoub AF: Validation and reproducibility of a high-resolution three-dimensional facial imaging system. *Br J Oral Maxillofac Surg.* 2008;46:27–32.
15. Krimmel M, Kluba S, Bacher M, Dietz K, and Reinert S: Digital surface photogrammetry for anthropometric analysis of the cleft infant face. *Cleft Palate Craniofac J.* 2006;43: 350–355.
16. MacQueen JB: Some methods for classification and analysis of multivariate observations. *Proceedings of Fifth Berkeley Symposium on Mathematical Statistics and Probability*, Vol. 1. University of California Press, Berkeley, CA: pp. 281–297, 1967.

Received on June 19, 2013  
in final form, July 30, 2013

Reviewed by:  
David Geller  
Ariel Berlinski

Address correspondence to:  
Dr. Israel Amirav  
Ziv Medical Center  
Faculty of Medicine  
Bar-Ilan University  
Safed  
Israel

E-mail: amirav@012.net.il